Supporting Information for

Porous Gold Nanocluster Decorated Manganese Monoxide Nanocomposites for Microenviroment-Activatable MR/Photoacoustic/CT Tumor Imaging

Yu Liu[a,b], Xiaolin Lv[c], Heng Liu[d], Zijian Zhou[a], Jianpan Huang[e], Shenglan Lei[c], Shuhui Cai[c], Zhong Chen[e], Yanli Guo[b], Zhiwei Chen[e], Xi Zhou[c]*, and Liming Nie[a]**

[a]State Key Laboratory of Molecular Vaccinology and Molecular Diagnosis & Center for Molecular Imaging and Translational Medicine, School of Public Health, Xiamen University, Xiamen, 361102, People's Republic of China. Email: nielm@xmu.edu.cn

[b]Department of Ultrasound, Southwest Hospital, Army Medical University, Chongqing, 400038, People's Republic of China

[c]Key Laboratory of Biomedical Engineering of Fujian Province University/Research Center of Biomedical Engineering of Xiamen, Department of Biomaterials, College of Materials, Xiamen University, Xiamen, 361100, People's Republic of China. Email: xizhou@xmu.edu.cn

[d] Department of Radiology, Institute of Surgery Research, Daping Hospital, Army Medical University, Chongqing, 400042, People's Republic of China

[e] Department of Electronic Science, Fujian Provincial Key Laboratory of Plasma and Magnetic Resonance Research, Xiamen University, Xiamen, 361000, People's Republic of China. Email: chenzhiwei@xmu.edu.cn

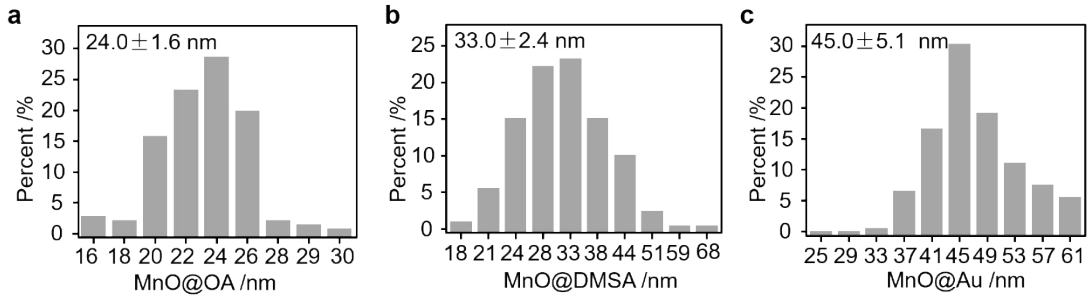

Figure S1. Size distribution analysis of (a) MnO@OA, (b) MnO@DMSA and (c) MnO@Au NCs on TEM images. buffer for different time points. The insets show corresponding PA images. TEM images of MnO@Au NCs incubated in pH=5.4 buffer for (c) 0 h and (d) 12 h.

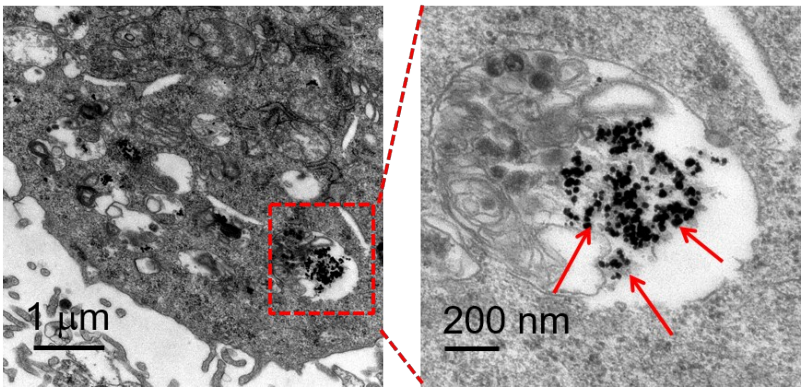

Figure S2. Representative TEM images of $HepG_2$ cells incubated with 150 μg/mL MnO@Au NCs for 6 h. Scale bar, 1 μm (left) and 200 nm (right).

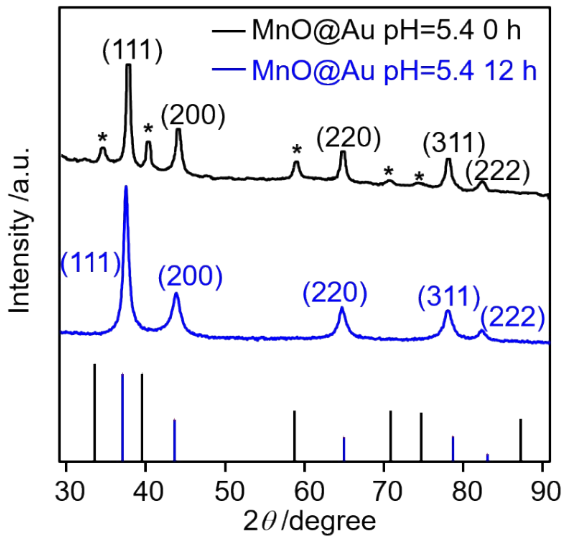

Figure S3. XRD patterns of MnO@Au NCs incubated with pH=5.4 buffer for 0 h and 12 h, respectively.

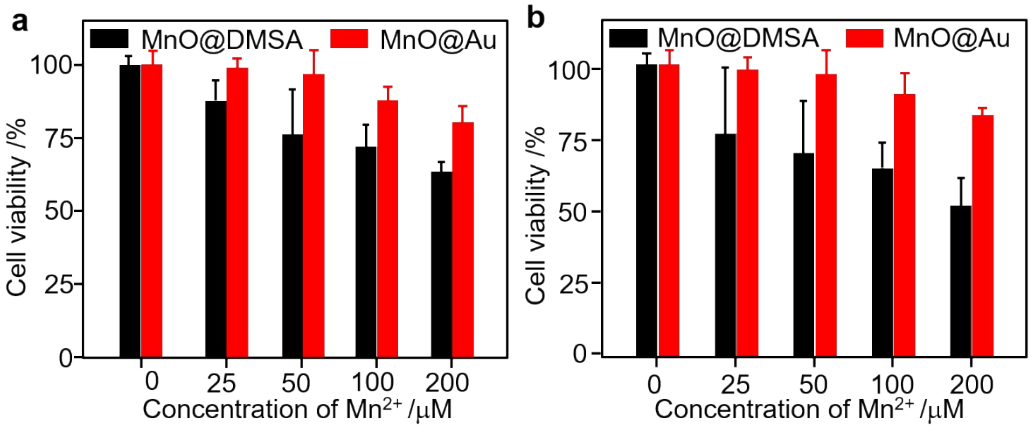

Figure S4. *In vitro* cytotoxicity assay of Hela cells (a) and $HepG_2$ cells (b) treated with various concentrations of MnO@DMSA and MnO@Au NCs for 24 h.

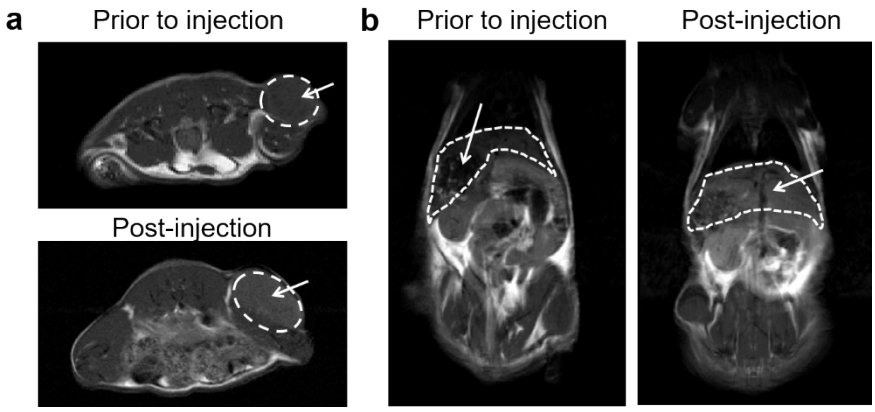

Figure S5. *In vivo* MRI of $HepG_2$ tumor-bearing mice at different time points after intravenous injection of MnO@Au NCs (200 μL, 2 mg/mL). (a) prior to injection (upper) and 24 h post-injection (lower). (b) Mouse liver prior to injection (left) and 4 h post-injection(right) after intravenous injection of MnO@Au NCs (200 μL, 2 mg/mL).

Colloids and Surfaces A: Physicochemical and Engineering Aspects

Volume 302, Issues 1–3, 20 July 2007, Pages 483-487

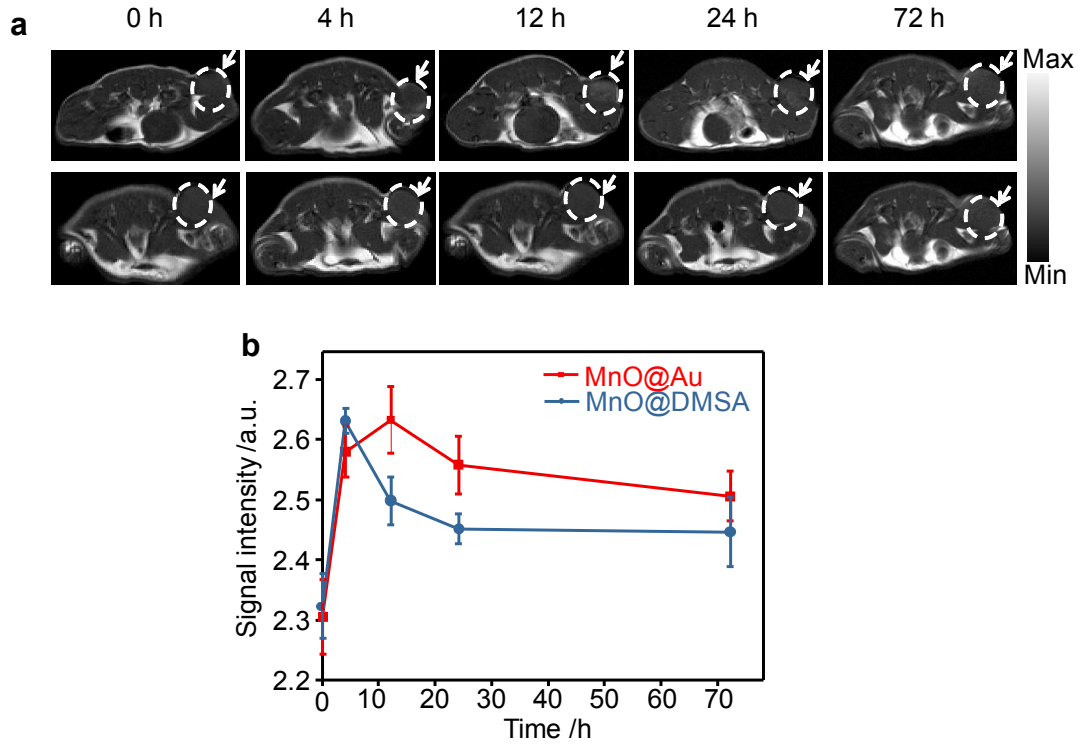

Figure S6 (a) Time-dependent T1-weighted MR images of 4T1 tumor-bearing mice after intravenous injection of 200 μL of 2 mg/mL MnO@Au NCs (upper row) and MnO@DMSA (lower row) and (b) corresponding signal intensity analysis. Mean values±s.d; n =3.

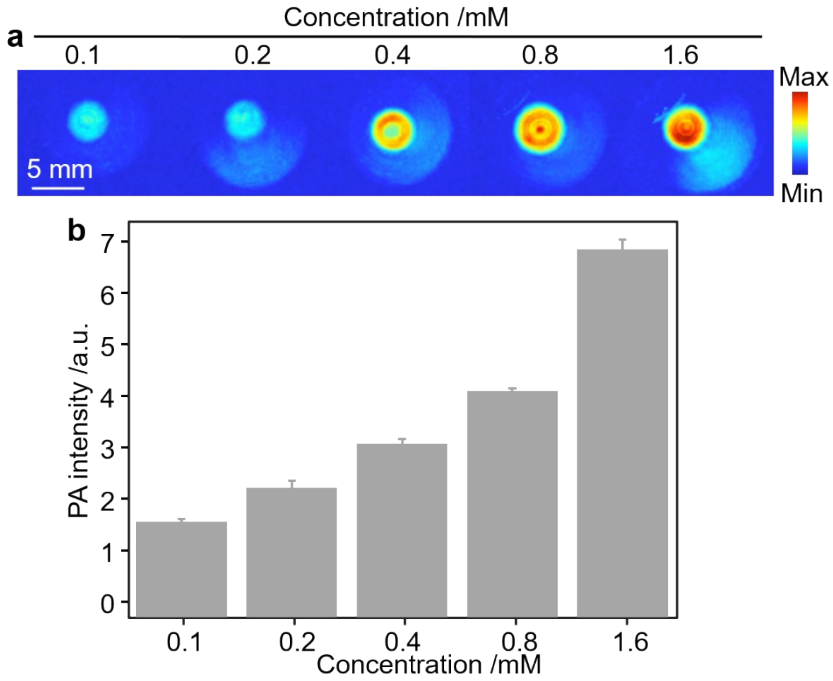

Figure S7. (a) Photoacoustic images of MnO@Au NCs with different Au molar concentrations. (b) The corresponding photoacoustic signal intensity analysis from Figure a.

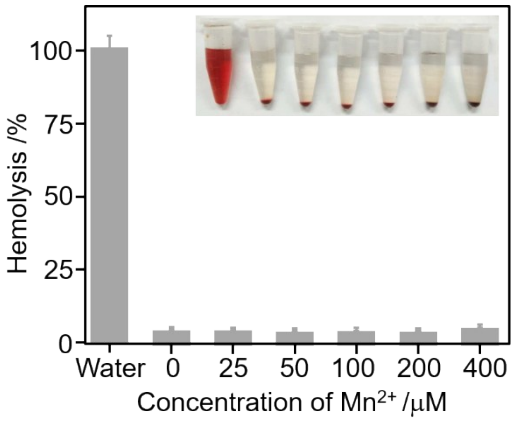

Figure S8. Hemolysis analysis of mouse RBCs (2.5%, v/v) after treated with various concentrations of MnO@Au NCs.

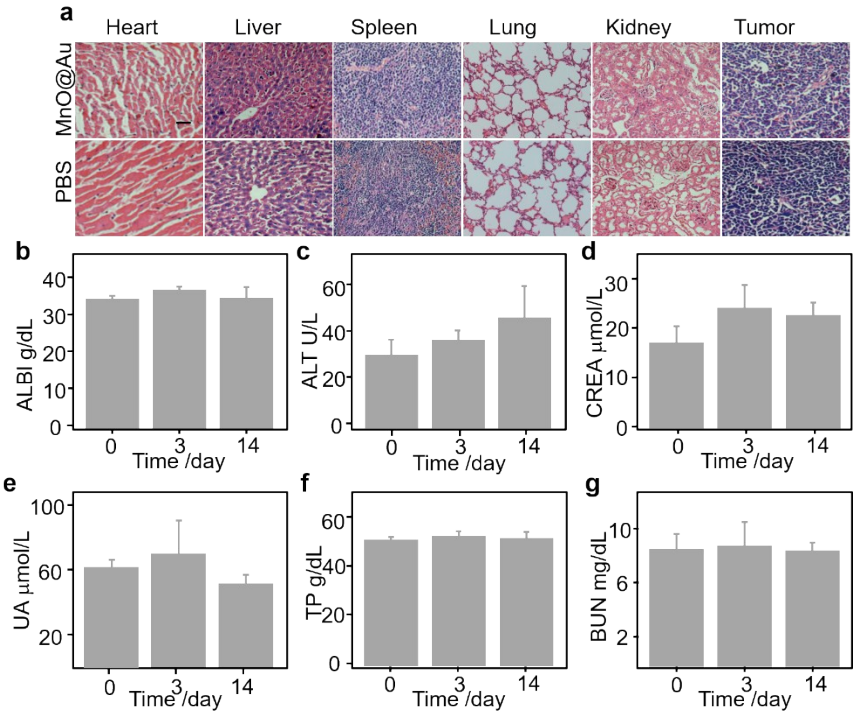

Figure S9. (a) H&E staining of major organs including heart, liver, spleen, lung, kidney and tumor of mice after intravenous injection of PBS (control) or MnO@Au NCs for 14 days. Scale bar, 50 μm. (b) Serum levels of albumin (ALB), (c) alanine aminotransferase (ALT), (d) crea creatinine (CREA), (e) alkaline phosphatase (ALP), (f) uric acid (UA), and (g) total protein (TP) at different time points after intravenous injection of MnO@Au NCs.